

# Dark Photon Dark Matter in Quantum Electromagnetodynamics and Detection at Haloscope Experiments

Tong Li,<sup>1,\*</sup> Rui-Jia Zhang,<sup>1,†</sup> and Chang-Jie Dai<sup>1,‡</sup>

<sup>1</sup>*School of Physics, Nankai University, Tianjin 300071, China*

## Abstract

The ultralight dark photon is one of intriguing dark matter candidates. The interaction between the visible photon and dark photon is introduced by the gauge kinetic mixing between the field strength tensors of the Abelian gauge groups in the Standard Model and dark sector. The relativistic electrodynamics was generalized to quantum electromagnetodynamics (QEMD) in the presence of both electric and magnetic charges. The photon is described by two four-potentials corresponding to two  $U(1)$  gauge groups and satisfying non-trivial commutation relations. In this work, we construct the low-energy dark photon-photon interactions in the framework of QEMD and obtain new dark photon-photon kinetic mixings. The consequent field equations and the new Maxwell's equations are derived in this framework. We also investigate the detection strategies of dark photon as light dark matter as well as the generic kinetic mixings at haloscope experiments.

arXiv:2407.01070v1 [hep-ph] 1 Jul 2024

---

\* [litong@nankai.edu.cn](mailto:litong@nankai.edu.cn)

† [zhangruijia@mail.nankai.edu.cn](mailto:zhangruijia@mail.nankai.edu.cn)

‡ [daichangjie@mail.nankai.edu.cn](mailto:daichangjie@mail.nankai.edu.cn)

## I. INTRODUCTION

The numerous candidates of dark matter (DM) motivate us to search for potential hidden particles in a wide range of mass scale. The dark photon (DP, or called hidden photon) [1, 2] is an appealing candidate of ultralight bosonic DM [3–5] (see a recent review Ref. [6] and references therein). It is a spin-one field particle gauged by an Abelian group in dark sector. The interaction between the visible photon and the dark photon is through the gauge kinetic mixing between the field strength tensors of the Standard Model (SM) electromagnetic gauge group  $U(1)_{\text{EM}}$  and the dark Abelian gauge group  $U(1)_D$  below the electroweak scale

$$\mathcal{L} \supset -\frac{1}{4}F^{\mu\nu}F_{\mu\nu} - \frac{1}{4}F_D^{\mu\nu}F_{D\mu\nu} - \frac{\epsilon}{2}F^{\mu\nu}F_{D\mu\nu} + \frac{1}{2}m_D^2 A_D^\mu A_{D\mu} , \quad (1)$$

where  $F^{\mu\nu}$  ( $F_D^{\mu\nu}$ ) is the SM (dark) field strength, and  $A_D$  is the dark gauge boson with mass  $m_D$ . Suppose the SM particles are uncharged under the dark gauge group, this kinetic mixing  $\epsilon \ll 1$  is generated by integrating out new heavy particles charged under both gauge groups at loop level. The two gauge fields can be rotated to get rid of the mixing and as a result, the SM matter current gains a shift by  $A_\mu \rightarrow A_\mu - \epsilon A_{D\mu}$ . Based on the framework of quantum electrodynamics (QED), the electromagnetic signals from the source of dark photon DM can be searched for in terrestrial experiments [4, 7–17].

The description of relativistic electrodynamics may not be as simple as QED theory. The magnetic monopole is one of the most longstanding and mysterious topics in history [18–26]. In 1960's, J. S. Schwinger and D. Zwanziger developed a generalized electrodynamics with monopoles in the presence of both electric and magnetic charges, called quantum electromagnetodynamics (QEMD) [27–29]. The characteristic feature of QEMD is to substitute the  $U(1)_{\text{EM}}$  gauge group by two  $U(1)$  gauge groups to introduce both electric and magnetic charges. Two four-potentials  $A_\mu$  and  $B_\mu$  (instead of only one  $A_\mu$  in QED) are introduced corresponding to the two  $U(1)$  gauge groups (called  $U(1)_A$  and  $U(1)_B$  below), respectively. They formally built a local Lagrangian density, a non-trivial form of equal-time canonical commutation relations and resulting Lagrangian field equations in a local quantum field theory. Zwanziger et al. also proved that the right degrees of freedom of physical photon are preserved and the Lorentz invariance is not violated in this theory [30–32]. Recently, based on the framework of QEMD, it was pointed out that more generic axion-photon interactions may arise and there appeared quite a few studies of them in theory [32–35] and phenomenology [12, 36–42].

In this work, we construct the dark photon-photon interactions in the framework of QEMD and investigate the relevant detection strategies of light dark photon DM. We introduce new heavy fermions  $\psi$  charged under the four electromagnetic  $U(1)$  groups, i.e.,  $U(1)_A \times U(1)_B$  in visible sector and  $U(1)_{A_D} \times U(1)_{B_D}$  in dark sector. The covariant derivative of  $\psi$  fermion in the kinetic term is then given by

$$i\bar{\psi}\gamma^\mu D_\mu\psi = i\bar{\psi}\gamma^\mu(\partial_\mu - eq_\psi A_\mu - gg_\psi B_\mu - e_D q_{D\psi} A_{D\mu} - g_D g_{D\psi} B_{D\mu})\psi , \quad (2)$$

where  $A_\mu, B_\mu$  ( $A_{D\mu}, B_{D\mu}$ ) are the potentials in the visible (dark) sector, and they are multiplied by the corresponding electric and magnetic charges. The visible photon is described by the two four-potentials  $A_\mu, B_\mu$  in the visible sector, and the dark photon is gauged under either QED (with only  $A_{D\mu}$ ) or QEMD (with both  $A_{D\mu}$  and  $B_{D\mu}$ ) in dark sector. After integrating out the new fermions  $\psi$  in vacuum polarization diagrams of the four potentials, one can obtain the new kinetic mixings between dark photon and visible photon. We show their low-energy Lagrangian and the consequent field equations which are equivalent to new Maxwell's equations of dark photon. Based on the new Maxwell's equations, we also study the detection strategies through haloscope experiments to search for the light dark photon DM in this framework as well as the new kinetic mixings.

This paper is organized as follows. In Sec. II, we introduce the QEMD theory and the effective Lagrangian of dark photon and visible photon in QEMD framework. In Sec. III, we show the generic kinetic mixing terms in the Lagrangian. The consequent field equations and the new Maxwell's equations are then derived in this framework. We discuss the setup and signal power of haloscope experiments for the generic kinetic mixings and dark photon DM in Sec. IV. We also show the sensitivity of haloscope experiments to each kinetic mixing or dark photon DM component. Our conclusions are drawn in Sec. V.

## II. FORMALISM OF PHOTON AND DARK PHOTON IN QEMD FRAMEWORK

In this section, we first describe the framework of QEMD theory and then introduce the necessary ingredients for constructing the extended dark photon-photon interactions based on QEMD.

To properly build a relativistic electrodynamics in the presence of magnetic monopole, a reliable method is to introduce two four-potentials  $A_\mu$  and  $B_\mu$  corresponding to two  $U(1)$  gauge groups  $U(1)_A$  and  $U(1)_B$ , respectively [27–29]. Both the electric and magnetic charges are inherently brought into the same theoretical framework. The general Maxwell's equations in the presence of electric and magnetic currents are

$$\partial_\mu F^{\mu\nu} = j_e^\nu, \quad \partial_\mu F^{d\ \mu\nu} = j_m^\nu, \quad (3)$$

where the Hodge dual of field strength  $F^{\mu\nu}$  is  $F^{d\ \mu\nu} = \frac{1}{2}\epsilon^{\mu\nu\rho\sigma}F_{\rho\sigma}$  with  $\epsilon_{0123} = +1$ , and the currents are conserved with  $\partial_\mu j_e^\mu = \partial_\mu j_m^\mu = 0$ . The general solutions to the above equations are

$$F = \partial \wedge A - (n \cdot \partial)^{-1} (n \wedge j_m)^d, \quad (4)$$

$$F^d = \partial \wedge B + (n \cdot \partial)^{-1} (n \wedge j_e)^d, \quad (5)$$

where  $n^\mu = (0, \vec{n})$  is an arbitrary space-like vector, the integral operator  $(n \cdot \partial)^{-1}$  satisfies  $n \cdot \partial (n \cdot \partial)^{-1}(x) = \delta^4(x)$  and we define  $(X \wedge Y)^{\mu\nu} \equiv X^\mu Y^\nu - X^\nu Y^\mu$  for any four-vectors  $X$  and  $Y$ . The above field strength tensors satisfy

$$n \cdot F = n \cdot (\partial \wedge A), \quad n \cdot F^d = n \cdot (\partial \wedge B). \quad (6)$$

Using the identity  $G = (1/n^2)[(n \wedge (n \cdot G)) - (n \wedge (n \cdot G^d))^d]$  for any antisymmetric tensor  $G$ , one can rewrite  $F$  and  $F^d$  only in terms of potentials

$$F = \frac{1}{n^2}(n \wedge [n \cdot (\partial \wedge A)] - n \wedge [n \cdot (\partial \wedge B)]^d), \quad (7)$$

$$F^d = \frac{1}{n^2}(n \wedge [n \cdot (\partial \wedge A)]^d + n \wedge [n \cdot (\partial \wedge B)]). \quad (8)$$

After substituting them into Eq. (3), we obtain the Maxwell's equations

$$\frac{n \cdot \partial}{n^2}(n \cdot \partial A^\mu - \partial^\mu n \cdot A - n^\mu \partial \cdot A - \epsilon_{\nu\rho\sigma}^\mu n^\nu \partial^\rho B^\sigma) = j_e^\mu, \quad (9)$$

$$\frac{n \cdot \partial}{n^2}(n \cdot \partial B^\mu - \partial^\mu n \cdot B - n^\mu \partial \cdot B + \epsilon_{\nu\rho\sigma}^\mu n^\nu \partial^\rho A^\sigma) = j_m^\mu. \quad (10)$$

These Maxwell's equations can be realized by the local Lagrangian of photon as follows [29]

$$\begin{aligned} \mathcal{L}_P = & -\frac{1}{2n^2}[n \cdot (\partial \wedge A)] \cdot [n \cdot (\partial \wedge B)]^d + \frac{1}{2n^2}[n \cdot (\partial \wedge B)] \cdot [n \cdot (\partial \wedge A)]^d \\ & -\frac{1}{2n^2}[n \cdot (\partial \wedge A)]^2 - \frac{1}{2n^2}[n \cdot (\partial \wedge B)]^2 - j_e \cdot A - j_m \cdot B + \mathcal{L}_G, \end{aligned} \quad (11)$$

where  $\mathcal{L}_G = (1/2n^2)\{[\partial(n \cdot A)]^2 + [\partial(n \cdot B)]^2\}$  is a gauge fixing term. One can rewrite it in terms of canonical variables and get the non-trivial commutation relations between the two four-potentials [29]

$$[A^\mu(t, \vec{x}), B^\nu(t, \vec{y})] = i\epsilon_{\kappa 0}^{\mu\nu} n^\kappa (n \cdot \partial)^{-1}(\vec{x} - \vec{y}), \quad (12)$$

$$[A^\mu(t, \vec{x}), A^\nu(t, \vec{y})] = [B^\mu(t, \vec{x}), B^\nu(t, \vec{y})] = -i(g_0^\mu n^\nu + g_0^\nu n^\mu)(n \cdot \partial)^{-1}(\vec{x} - \vec{y}). \quad (13)$$

The right number of photon degrees of freedom is preserved due to the constraints from the above equations of motion, gauge condition and equal-time commutation relations. We notice the other important identity between two antisymmetric tensors  $G$  and  $H$

$$\text{tr}(G \cdot H) = G^{\mu\nu} H_{\nu\mu} = \frac{2}{n^2}[-(n \cdot G)(n \cdot H) + (n \cdot G^d)(n \cdot H^d)]. \quad (14)$$

The QEMD Lagrangian of visible photon is then rewritten as

$$\mathcal{L}_P = \frac{1}{4}\text{tr}(F \cdot (\partial \wedge A)) + \frac{1}{4}\text{tr}(F^d \cdot (\partial \wedge B)) - j_e \cdot A - j_m \cdot B + \mathcal{L}_G. \quad (15)$$

The same result can also be obtained based on Schwinger's phenomenological source theory (PST) [43, 44]. PST introduces source function to express the particles involved in a collision. The vacuum amplitude between two types of sources yields the  $S$  matrix element. For the theory of magnetic charge, based on PST, Ref. [45] showed the same action of photon as Eq. (15) in QEMD theory. Similarly, the Lagrangian of massive dark photon gains the following form

$$\begin{aligned} \mathcal{L}_{DP} = & -\frac{1}{2n^2}[n \cdot (\partial \wedge A_D)] \cdot [n \cdot (\partial \wedge B_D)]^d + \frac{1}{2n^2}[n \cdot (\partial \wedge B_D)] \cdot [n \cdot (\partial \wedge A_D)]^d \\ & -\frac{1}{2n^2}[n \cdot (\partial \wedge A_D)]^2 - \frac{1}{2n^2}[n \cdot (\partial \wedge B_D)]^2 + \frac{1}{2}m_D^2 A_D^\mu A_{D\mu} + \frac{1}{2}m_D^2 B_D^\mu B_{D\mu} + \mathcal{L}_{GD} \\ = & \frac{1}{4}\text{tr}(F_D \cdot (\partial \wedge A_D)) + \frac{1}{4}\text{tr}(F_D^d \cdot (\partial \wedge B_D)) + \frac{1}{2}m_D^2 A_D^\mu A_{D\mu} + \frac{1}{2}m_D^2 B_D^\mu B_{D\mu} + \mathcal{L}_{GD} \end{aligned} \quad (16)$$

where  $\mathcal{L}_{GD}$  denotes the gauge fixing term for DP.

### III. DARK PHOTON-PHOTON INTERACTIONS AND FIELD EQUATIONS

Inspired by the two potential terms in either  $\mathcal{L}_P$  or  $\mathcal{L}_{DP}$ , we can build the low-energy dark photon-photon kinetic mixing interactions as follows

$$\begin{aligned} \mathcal{L}_{DP-P} = & \frac{\epsilon_1}{2} \text{tr}(F \cdot (\partial \wedge A_D)) + \frac{\epsilon_1}{2} \text{tr}(F^d \cdot (\partial \wedge B_D)) \\ & + \frac{\epsilon_2}{2} \text{tr}(F^d \cdot (\partial \wedge A_D)) - \frac{\epsilon_2}{2} \text{tr}(F \cdot (\partial \wedge B_D)) . \end{aligned} \quad (17)$$

This Lagrangian is equivalent to the one with the substitution of  $A \leftrightarrow A_D$  and  $B \leftrightarrow B_D$ . They contribute to the same equations of motion. The two mixing parameters  $\epsilon_1$  and  $\epsilon_2$  can be obtained by integrating out the new heavy fermion  $\psi$  in vacuum polarization diagram of the potentials in visible and dark sectors. Suppose the fermion  $\psi$  is only charged in  $U(1)_{A_D}$  group in dark sector, the above Lagrangian is simplified as

$$\mathcal{L}'_{DP-P} = \frac{\epsilon_1}{2} \text{tr}(F \cdot (\partial \wedge A_D)) + \frac{\epsilon_2}{2} \text{tr}(F^d \cdot (\partial \wedge A_D)) , \quad (18)$$

where the terms with potential  $B_D$  in  $\mathcal{L}_{DP-P}$  vanish.

We next apply the Euler-Lagrange equation to the above DP-P Lagrangian  $\mathcal{L}_{DP-P}$  and then obtain the field equations of photon as

$$\partial_\mu F^{\mu\nu} + \epsilon_1 \partial_\mu F_D^{\mu\nu} - \epsilon_2 \partial_\mu F_D^{d\mu\nu} = j_e^\nu , \quad (19)$$

$$\partial_\mu F^{d\mu\nu} + \epsilon_1 \partial_\mu F_D^{d\mu\nu} + \epsilon_2 \partial_\mu F_D^{\mu\nu} = j_m^\nu . \quad (20)$$

The equations of motion for dark photon are

$$\partial_\mu F_D^{\mu\nu} + m_D^2 A_D^\nu + \epsilon_1 \partial_\mu F^{\mu\nu} + \epsilon_2 \partial_\mu F^{d\mu\nu} = 0 , \quad (21)$$

$$\partial_\mu F_D^{d\mu\nu} + m_D^2 B_D^\nu + \epsilon_1 \partial_\mu F^{d\mu\nu} - \epsilon_2 \partial_\mu F^{\mu\nu} = 0 . \quad (22)$$

After inserting the dark photon equations into Eqs. (19) and (20), we obtain the modified Maxwell's equations

$$\partial_\mu F^{\mu\nu} = \epsilon_1 m_D^2 A_D^\nu - \epsilon_2 m_D^2 B_D^\nu , \quad (23)$$

$$\partial_\mu F^{d\mu\nu} = \epsilon_1 m_D^2 B_D^\nu + \epsilon_2 m_D^2 A_D^\nu , \quad (24)$$

where the  $\mathcal{O}(\epsilon_{1,2}^2)$  terms are neglected, and the primary electromagnetic fields driven by the static currents and charges have been subtracted here. Note that the right-handed sides of Eqs. (23) and (24) are the linear combinations of  $A_D$  and  $B_D$ . We perform an  $O(2)$  transformation

$$\begin{pmatrix} \tilde{A}_D \\ \tilde{B}_D \end{pmatrix} = \begin{pmatrix} \cos \varphi & -\sin \varphi \\ \sin \varphi & \cos \varphi \end{pmatrix} \begin{pmatrix} A_D \\ B_D \end{pmatrix} , \quad (25)$$

where  $\cos \varphi = \epsilon_1 / \sqrt{\epsilon_1^2 + \epsilon_2^2}$  and  $\sin \varphi = \epsilon_2 / \sqrt{\epsilon_1^2 + \epsilon_2^2}$ . The equations then become

$$\partial_\mu F^{\mu\nu} = \epsilon m_D^2 \tilde{A}_D^\nu , \quad (26)$$

$$\partial_\mu F^{d\ \mu\nu} = \epsilon m_D^2 \tilde{B}_D^\nu, \quad (27)$$

where the only mixing parameter is  $\epsilon = \sqrt{\epsilon_1^2 + \epsilon_2^2}$ . Corresponding to the Lagrangian  $\mathcal{L}'_{\text{DP-P}}$ , the above Maxwell's equations are simplified as

$$\partial_\mu F^{\mu\nu} = \epsilon_1 m_D^2 A_D^\nu, \quad (28)$$

$$\partial_\mu F^{d\ \mu\nu} = \epsilon_2 m_D^2 A_D^\nu, \quad (29)$$

where there is only  $A_D$  in dark sector and the two equations rely on  $\epsilon_1$  and  $\epsilon_2$ , respectively.

The modified Ampère's law and Faraday's law equations become

$$\vec{\nabla} \times \vec{\mathbb{B}} = \frac{\partial \vec{\mathbb{E}}}{\partial t} + \vec{j}_{eD}, \quad (30)$$

$$-\vec{\nabla} \times \vec{\mathbb{E}} = \frac{\partial \vec{\mathbb{B}}}{\partial t} + \vec{j}_{mD}, \quad (31)$$

where we use symbols “ $\mathbb{E}$ ” and “ $\mathbb{B}$ ” to denote the DP induced electric and magnetic fields, respectively. After applying the curl differential operator to the above equations, one obtains two second-order differential equations

$$\vec{\nabla}^2 \vec{\mathbb{E}} - \frac{\partial^2 \vec{\mathbb{E}}}{\partial t^2} = \frac{\partial \vec{j}_{eD}}{\partial t} + \vec{\nabla} \times \vec{j}_{mD}, \quad (32)$$

$$\vec{\nabla}^2 \vec{\mathbb{B}} - \frac{\partial^2 \vec{\mathbb{B}}}{\partial t^2} = \frac{\partial \vec{j}_{mD}}{\partial t} - \vec{\nabla} \times \vec{j}_{eD}, \quad (33)$$

where we take  $A_D^0 = 0$  or  $\tilde{A}_D^0 = \tilde{B}_D^0 = 0$ , and only keep the spatial components of them [4]. Next, we consider two cases for the dark currents corresponding to the above two types of Maxwell's equations, respectively

$$\text{case I : } \begin{cases} \vec{j}_{eD} = \epsilon_1 m_D^2 \vec{A}_D, \\ \vec{j}_{mD} = \epsilon_2 m_D^2 \vec{A}_D, \end{cases} \quad \text{case II : } \begin{cases} \vec{j}_{eD} = \epsilon m_D^2 \vec{A}_D, \\ \vec{j}_{mD} = \epsilon m_D^2 \vec{\tilde{B}}_D. \end{cases} \quad (34)$$

The two cases also correspond to one-component ( $A_D$ ) DM scenario or two-component ( $\tilde{A}_D$  and  $\tilde{B}_D$ ) DM scenario. In these two cases, the local DM density [46, 47] is given by

$$\rho_0 = 0.45 \text{ GeV cm}^{-3} = \begin{cases} \frac{1}{2} m_D^2 |\vec{A}_D|^2 & \text{case I,} \\ \frac{1}{2} m_D^2 (|\vec{A}_D|^2 + |\vec{\tilde{B}}_D|^2) & \text{case II.} \end{cases} \quad (35)$$

We adopt the scenario in Refs. [4, 7] to ensure that the dark photon field is along a fixed direction  $\vec{k}$ . As a result,  $\vec{\nabla} \times \vec{j}_{eD} = \vec{\nabla} \times \vec{j}_{mD} = 0$ . In case II, we define the ratio of two-component DM percentages as

$$\frac{|\vec{A}_D|^2}{|\vec{\tilde{B}}_D|^2} = \frac{x}{1-x}, \quad (36)$$

where  $0 < x < 1$ . Then, the DP DM fields can be expressed as follows

$$\text{case I: } \vec{A}_D = \frac{\sqrt{2\rho_0}}{m_D} e^{-im_D t} \hat{k}, \quad \text{case II: } \begin{cases} \vec{A}_D = \frac{\sqrt{2\rho_0 x}}{m_D} e^{-im_D t} \hat{k} \\ \vec{B}_D = \frac{\sqrt{2\rho_0(1-x)}}{m_D} e^{-im_D t} \hat{k} \end{cases}, \quad (37)$$

One can see that in case I, the DM density is composed of  $A_D$  only. The two second-order differential equations are governed by two kinetic mixing parameters  $\epsilon_1$  and  $\epsilon_2$ , respectively. In case II, there is one free kinetic mixing parameter  $\epsilon$ . The two equations are induced by the two components of DM  $\vec{A}_D$  and  $\vec{B}_D$ , respectively.

#### IV. STRATEGY AND SENSITIVITY OF HALOSCOPE EXPERIMENTS

Next, we solve the above equations in terms of the DP DM fields, and examine the detection strategies in cavity haloscope experiment [4] or LC circuit experiment [7, 8]. Below we take case II as an illustrative investigation and solve the two equations governed by  $\vec{A}_D$  and  $\vec{B}_D$ , respectively. The results of case I can be easily obtained by taking the substitution  $\epsilon\sqrt{x} \rightarrow \epsilon_1$  or  $\epsilon\sqrt{1-x} \rightarrow \epsilon_2$ .

For the direction of DP DM, we assume  $\theta$  as the angle between the direction  $\vec{k}$  of the DP field and the  $z$  direction in the laboratory coordinate system [4]. We need to average the final result over all randomly pointing directions for  $\vec{k}$ .

##### A. cavity haloscope

We first revisit the solution of Eq. (32) in case II for cavity experiment. It is exactly the same Maxwell's equation induced by DP DM electrodynamics for conventional cavity experiment.

The electric field  $\vec{\mathbb{E}}(t, \vec{x})$  in microwave cavity can be decomposed as the superposition of the time-evolution functions  $e_n(t)$  and orthogonal modes  $\mathbb{E}_n(\vec{x})$

$$\vec{\mathbb{E}}(t, \vec{x}) = \sum_n e_n(t) \vec{\mathbb{E}}_n(\vec{x}), \quad (38)$$

where modes  $\vec{\mathbb{E}}_n(\vec{x})$  satisfy the Helmholtz equation  $\nabla^2 \vec{\mathbb{E}}_n + \omega_n^2 \vec{\mathbb{E}}_n = 0$  with the resonant frequency  $\omega_n$  being equal to the frequency of DP  $\omega_D \approx m_D$ . Plugging  $\vec{\mathbb{E}}(t, \vec{x})$  into Eq. (32) and considering the losses within cavity, we obtain the expansion coefficient  $e_n(t)$  as follows

$$\left( \frac{d^2}{dt^2} + \frac{\omega_D}{Q} \frac{d}{dt} + \omega_D^2 \right) e_n(t) = -\frac{\epsilon m_D^2}{C_n^{\mathbb{E}}} \int dV \vec{\mathbb{E}}_n^*(\vec{x}) \cdot \partial_t \vec{A}_D, \quad (39)$$

where the normalization coefficients are defined as  $C_n^{\mathbb{E}} = \int dV |\vec{\mathbb{E}}_n(\vec{x})|^2$  and  $Q$  denotes quality factor. When assuming  $e_n(t) = e_{n,0} e^{-i\omega t}$ , the coefficient  $e_{n,0}$  is given by

$$e_{n,0} = \frac{(\omega_D^2 - \omega^2 + i\frac{\omega\omega_D}{Q})}{(\omega_D^2 - \omega^2)^2 + \frac{\omega^2\omega_D^2}{Q^2}} \Big|_{\omega \approx \omega_D} \times \left( -\frac{\epsilon m_D^2}{C_n^{\mathbb{E}}} \right) \int dV \vec{\mathbb{E}}_n^* \cdot \partial_t \vec{A}_D$$

$$= -i \frac{\epsilon Q}{C_n^{\mathbb{E}}} \times \int dV \vec{\mathbb{E}}_n^*(\vec{x}) \cdot \partial_t \vec{A}_D. \quad (40)$$

The output power in the cavity can be obtained in terms of the energy stored in the cavity  $U$  and the quality factor

$$P_{\text{DP}}^{\mathbb{E}} = \kappa \frac{U}{Q} \omega_D = \kappa \frac{\omega_D}{Q} \frac{|e_{n,0}|^2}{2} \int dV |\vec{\mathbb{E}}_n(\vec{x})|^2 = \frac{\kappa}{2} \epsilon^2 m_D Q V |\partial_t \vec{A}_D|^2 G^{\mathbb{E}} \cos^2 \theta, \quad (41)$$

where  $\kappa$  is the cavity coupling factor depending on the experimental setup,  $|\partial_t \vec{A}_D|^2 = 2\rho_0 x$ , and the form factor depending on the geometry of cavity is

$$G^{\mathbb{E}} = \frac{|\int dV \vec{\mathbb{E}}_n^*(\vec{x}) \cdot \vec{z}|^2}{V \int dV |\vec{\mathbb{E}}_n(\vec{x})|^2}. \quad (42)$$

After averaging over all possible directions of DP, compared to the axion cavity detection, the form factor here should be multiplied by  $\langle \cos^2 \theta \rangle = \int \cos^2 \theta d\Omega / \int d\Omega = 1/3$ .

It was demonstrated that for the detection of the DP field, similar to the axion search in cavity experiments, the  $\text{TM}_{010}$  mode has the largest coupling to DP with the electric field along the  $\vec{z}$ -axis. In this case, the theoretical value of the form factor for ideal cylindrical cavity is  $G^{\mathbb{E}} \approx 0.69$  and the value for ADMX with tuning rods is  $G^{\mathbb{E}} \approx 0.455$  [47]. The signal power in axion cavity experiments can be shown as

$$P_{\text{axion}}^{\mathbb{E}} = \kappa \left[ g_{a\gamma\gamma}^2 \frac{|\mathbb{B}_0|^2}{m_a} \right] \rho_0 Q V G^{\mathbb{E}}, \quad (43)$$

where  $|\mathbb{B}_0|$  denotes the magnitude of the external static magnetic field. Taking  $P_{\text{DP}}^{\mathbb{E}} = P_{\text{axion}}^{\mathbb{E}}$  yields the relation

$$\epsilon^2 m_D x \langle \cos^2 \theta \rangle = g_{a\gamma\gamma}^2 \frac{|\mathbb{B}_0|^2}{m_a}. \quad (44)$$

The constraints on the axion-photon coupling  $g_{a\gamma\gamma}$  from the existing axion cavity experiments can be converted to constrain the parameter  $\epsilon\sqrt{x}$  for DP. Fig. 1 shows the sensitivity of cavity haloscope experiment to kinetic mixing  $\epsilon\sqrt{x}$  (or  $\epsilon_1$ ) as a function of  $m_D$ . For  $\epsilon\sqrt{x}$ , we show the converted limits (gray) from axion cavity experiments according to Eq. (44) as well as direct DP search limits (red) from WISPDMM [9], SRF cavity [16], SQuAD [48] and APEX [17].

Similarly, we can follow the same procedure to obtain the solution of Eq. (33) for the emission power of magnetic field modes  $\vec{\mathbb{B}}_n(\vec{x})$  induced by  $\partial_t \vec{B}_D$

$$P_{\text{DP}}^{\mathbb{B}} = \frac{\kappa}{2} \epsilon^2 m_D Q V |\partial_t \vec{B}_D|^2 G^{\mathbb{B}} \cos^2 \theta = \kappa \epsilon^2 m_D (1-x) \rho_0 Q V G^{\mathbb{B}} \cos^2 \theta, \quad (45)$$

$$G^{\mathbb{B}} = \frac{|\int dV \vec{\mathbb{B}}_n^*(\vec{x}) \cdot \vec{z}|^2}{V \int dV |\vec{\mathbb{B}}_n(\vec{x})|^2}. \quad (46)$$

Next, we discuss the feasibility of DP field  $\vec{B}_D$  detection. It turns out that one needs the magnetic field modes along the  $\vec{z}$ -axis, corresponding to the TE modes. In an ideal cylindrical cavity, the



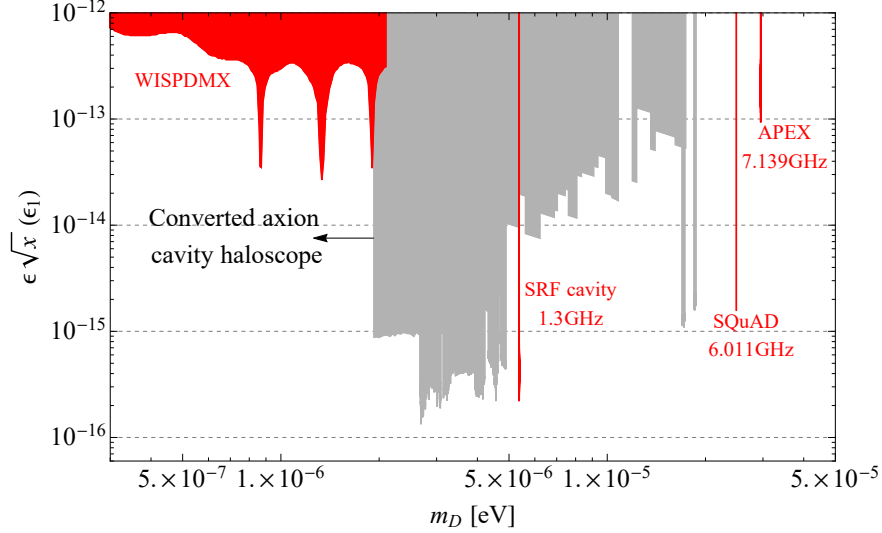


FIG. 1. The sensitivity of cavity haloscope experiment to kinetic mixing  $\epsilon\sqrt{x}$  ( $\epsilon_1$ ). For the converted results in gray, we take the limits of axion coupling  $g_{a\gamma\gamma}$  from the AxionLimits repository [50]. The direct DP search limits from WISPDPMX [9], SRF cavity [16], SQuAD [48] and APEX [17] are also shown in red.

form factor of  $TE_{011}$  mode is canceled over the radial integral from 0 to the radius. The higher-order  $TE_{111}$  mode exhibits periodic symmetry along the direction of azimuthal angle  $\phi$ . This causes the response to dark photon to be canceled over the integral from 0 to  $2\pi$ . To avoid the cancellation, taking  $TE_{111}$  mode for illustration, we need imperfectly symmetric field distribution over the azimuthal angle direction within the cavity. In the practical setup of cavity experiment, tuning rods are placed within the cylindrical cavity in order to tune the mode. For instance, in the ADMX experiment, two copper rods are put inside the cavity for frequency tuning. As indicated in Ref. [49], the tuning rods rotate around a fixed center and then the field distribution in cavity transforms asymmetrically over a full scan cycle. Here, a reasonable modification for the  $TE_{111}$  mode is to take only one half of the original cylindrical cavity. We then partially integrate the magnetic field and calculate the form factors. Specifically, after integrating the azimuthal angle from 0 to  $\pi$ , the analytical result of the form factor  $G^{\mathbb{B}}$  corresponding to  $TE_{111}$  mode is  $(128/\pi^4 x_{1,1}'^2) \times (c_1^2/c_2) \approx 0.61$ , where  $c_1 = \int_0^{x_{1,1}'} dx x J_1(x)$  and  $c_2 = \int_0^{x_{1,1}'} dx x J_1^2(x)$  with  $x_{m,n}'$  being the  $n$ -th zero point of the first derivative of Bessel function  $J_m(x)$ . It is close to the form factor of  $TM_{010}$  mode. We leave the detailed electromagnetic simulation in a future work.

## B. LC circuit

For LC circuit experiment, one needs to solve the DP Maxwell's equations with electromagnetic shielding [8]. We take the shield as a conducting or superconducting hollow cylinder of radius  $R$  along the  $\hat{z}$  direction in cylindrical coordinates  $(\rho, \phi, z)$ . In our case, in the presence of  $\vec{j}_{eD}$  and  $\vec{j}_{mD}$ , both the induced electric field and magnetic field in  $z$  direction would respectively be

suppressed as a result of the electromagnetic shielding. That is to say the observed  $\vec{\mathbb{E}}$  and  $\vec{\mathbb{B}}$  fields should be solved under the boundary conditions  $\hat{z} \cdot \vec{\mathbb{E}} = \hat{z} \cdot \vec{\mathbb{B}} = 0$  on the surface with  $\rho = R$  [8]. The  $\vec{\mathbb{B}}$  and  $\vec{\mathbb{E}}$  along the  $\phi$  direction generated by the currents then become the dominant observable fields inside the shield.

The DP field is projected to the  $z$  direction below, and thus we have  $\vec{j}_{eD} = \epsilon m_D \sqrt{2\rho_0 x} e^{-im_D t} \cos \theta \hat{z}$  and  $\vec{j}_{mD} = \epsilon m_D \sqrt{2\rho_0(1-x)} e^{-im_D t} \cos \theta \hat{z}$ . For the current  $\vec{j}_{eD}$  induced by  $\vec{A}_D$ , we solve the following equations

$$\vec{\nabla}^2 \vec{\mathbb{E}} - \frac{\partial^2 \vec{\mathbb{E}}}{\partial t^2} = \frac{\partial \vec{j}_{eD}}{\partial t}, \quad (47)$$

$$\vec{\nabla} \times \vec{\mathbb{B}} = \frac{\partial \vec{\mathbb{E}}}{\partial t} + \vec{j}_{eD}. \quad (48)$$

The solution of observable  $\vec{\mathbb{E}}$  and  $\vec{\mathbb{B}}$  becomes

$$\begin{aligned} \vec{\mathbb{E}}_{\text{obs}} &= -i\epsilon \sqrt{2\rho_0 x} \cos \theta e^{-im_D t} \left(1 - \frac{J_0(m_D \rho)}{J_0(m_D R)}\right) \hat{z} \\ &\approx i\epsilon \sqrt{2\rho_0 x} \cos \theta e^{-im_D t} m_D^2 (R^2 - \rho^2) \hat{z}, \end{aligned} \quad (49)$$

$$\vec{\mathbb{B}}_{\text{obs}} = \epsilon \sqrt{2\rho_0 x} \cos \theta e^{-im_D t} \frac{J_1(m_D \rho)}{J_0(m_D R)} \hat{\phi} \approx \epsilon \sqrt{2\rho_0 x} \cos \theta e^{-im_D t} m_D \rho \hat{\phi}. \quad (50)$$

When  $x \rightarrow 1$ , it is exactly the same as the solution in Ref. [8]. An adjustable LC circuit is put inside a hollow conducting shield, and the inducting coil is wrapped around the  $\phi$  direction of the conductor to receive the driving magnetic field. When the resonant frequency of the LC circuit is tuned to the DP oscillation frequency, the observable magnetic field gives rise to the magnetic flux and the consequent current

$$\Phi_{\text{obs}} \approx Q \epsilon \sqrt{2\rho_0 x} \cos \theta m_D V, \quad I = \frac{\Phi_{\text{obs}}}{L}, \quad (51)$$

where  $Q \sim 10^6$  is the quality factor of the LC circuit,  $V$  is the volume of the inductor and  $L$  is the inductance of the inducting coil. The signal power is then given by

$$P_{\text{signal}} = \langle I^2 R_s \rangle \approx \frac{\rho_0 x Q \epsilon^2 \langle \cos^2 \theta \rangle m_D^3 V^2}{L} \approx \rho_0 x Q \epsilon^2 \langle \cos^2 \theta \rangle m_D^3 V^{5/3}, \quad (52)$$

where  $R_s = L m_D / Q$  is the resistance.

The equations for current  $\vec{j}_{mD}$  induced by  $\vec{B}_D$  are

$$\vec{\nabla}^2 \vec{\mathbb{B}} - \frac{\partial^2 \vec{\mathbb{B}}}{\partial t^2} = \frac{\partial \vec{j}_{mD}}{\partial t}, \quad (53)$$

$$-\vec{\nabla} \times \vec{\mathbb{E}} = \frac{\partial \vec{\mathbb{B}}}{\partial t} + \vec{j}_{mD}. \quad (54)$$

The solution is

$$\vec{\mathbb{B}}_{\text{obs}} = -i\epsilon \sqrt{2\rho_0(1-x)} \cos \theta e^{-im_D t} \left(1 - \frac{J_0(m_D \rho)}{J_0(m_D R)}\right) \hat{z}$$

$$\approx i\epsilon\sqrt{2\rho_0(1-x)}\cos\theta e^{-im_D t}m_D^2(R^2-\rho^2)\hat{z}, \quad (55)$$

$$\vec{\mathbb{E}}_{\text{obs}} = -\epsilon\sqrt{2\rho_0(1-x)}\cos\theta e^{-im_D t}\frac{J_1(m_D\rho)}{J_0(m_D R)}\hat{\phi} \approx -\epsilon\sqrt{2\rho_0(1-x)}\cos\theta e^{-im_D t}m_D\rho\hat{\phi}. \quad (56)$$

In this case, a superconducting shield is placed outside the electromagnetic detector. The magnetic field in  $z$  direction is suppressed due to the superconducting Meissner effect. A wire loop is put inside the cylindrical hole of the superconducting shield to conduct the induction current [36]. The LC circuit is then connected to the wire loop to enhance the signal power. The induction current is

$$I = \frac{2\pi R\mathbb{E}_{\text{obs}}(R)}{R_s} = \frac{2\pi R^2\epsilon\sqrt{2\rho_0(1-x)}\cos\theta m_D}{R_s}. \quad (57)$$

The signal power is then given by

$$P_{\text{signal}} = \langle I^2 R_s \rangle \approx \frac{\rho_0(1-x)Q\epsilon^2\langle\cos^2\theta\rangle m_D V^{4/3}}{L} \approx \rho_0(1-x)Q\epsilon^2\langle\cos^2\theta\rangle m_D V. \quad (58)$$

We adopt the cryogenic amplifier described in Ref. [51] to receive and amplify the signals. The thermal noise exists in circuit can be estimated as

$$P_{\text{noise}} = \kappa_B T_N \sqrt{\frac{\Delta f}{\Delta t}}, \quad (59)$$

where  $\kappa_B$  is the Boltzmann constant,  $T_N$  is the noise temperature,  $\Delta f = f/Q$  is the detector bandwidth and  $\Delta t$  is the observation time. We take one week of observation time and two setup benchmarks of volume  $V$ , inductance  $L$  and temperature  $T_N$  for both cases. An adjustable capacitance with a minimal value of 50 pF is taken, resulting a maximal frequency. To estimate the sensitivity of  $\epsilon\sqrt{x}$  or  $\epsilon\sqrt{1-x}$ , we require the signal-to-noise ratio (SNR) to satisfy

$$\text{SNR} = \frac{P_{\text{signal}}}{P_{\text{noise}}} > 3. \quad (60)$$

In Fig. 2, we show the sensitivity of LC circuit to  $\epsilon\sqrt{x}$  ( $\epsilon_1$ ) (red) and  $\epsilon\sqrt{1-x}$  ( $\epsilon_2$ ) (blue). The search potential of  $\vec{B}_D$  is more promising than that of  $\vec{A}_D$  at low frequencies. Some exclusion limits for light DP DM are also shown, including DM Pathfinder (green) [52], ADMX SLIC (purple) [53], Dark E-Field Radio Experiment (orange) [54] and (gray) [55].

## V. CONCLUSIONS

Dark matter and magnetic monopole are two of longstanding candidates of new physics beyond the SM. The ultralight dark photon is an intriguing bosonic dark matter. The interaction between the visible photon and dark photon is introduced by the gauge kinetic mixing between the field strength tensors of SM electromagnetic gauge group and dark Abelian gauge group. On the other hand, the relativistic electrodynamics was generalized to quantum electromagnetodynamics in the presence of both electric and magnetic charges. In QEMD theory, the physical photon is described by two four-potentials  $A_\mu$  and  $B_\mu$  corresponding to two  $U(1)$  gauge groups  $U(1)_A \times U(1)_B$ .

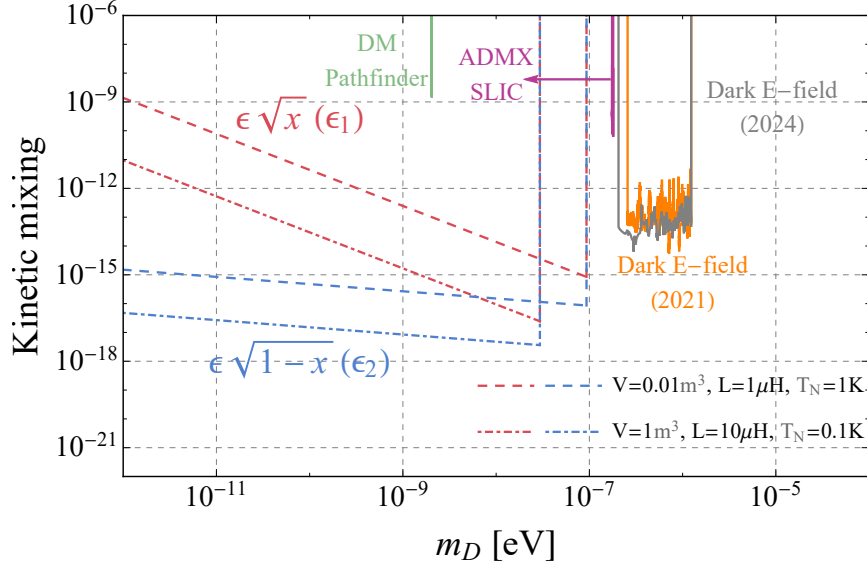


FIG. 2. The sensitivity of LC circuit to kinetic mixings  $\epsilon\sqrt{x}$  ( $\epsilon_1$ ) (red) and  $\epsilon\sqrt{1-x}$  ( $\epsilon_2$ ) (blue). We assume two setup benchmarks for both cases. Some existing limits for light DP DM are also shown, including DM Pathfinder (green) [52], ADMX SLIC (purple) [53], Dark E-Field Radio Experiment (orange) [54] and (gray) [55].

In this work, we construct the low-energy dark photon-photon interactions in the framework of QEMD. We introduce new heavy fermions charged under  $U(1)_A \times U(1)_B$  in visible sector and  $U(1)_{A_D} \times U(1)_{B_D}$  in dark sector. After integrating out the new fermions in vacuum polarization diagrams, the new dark photon-photon kinetic mixing interactions can be obtained. We derive the consequent field equations and the new Maxwell's equations in this framework. We also investigate the detection strategies of light dark photon DM as well as the generic kinetic mixings in cavity haloscope experiments and LC circuit experiments.

## ACKNOWLEDGMENTS

We would like to thank Yu Gao for useful discussions. T. L. is supported by the National Natural Science Foundation of China (Grant No. 12375096, 12035008, 11975129) and “the Fundamental Research Funds for the Central Universities”, Nankai University (Grants No. 63196013).

- 
- [1] B. Holdom, *Phys. Lett. B* **166**, 196 (1986).
  - [2] B. Holdom, *Phys. Lett. B* **178**, 65 (1986).
  - [3] A. E. Nelson and J. Scholtz, *Phys. Rev. D* **84**, 103501 (2011), [arXiv:1105.2812 \[hep-ph\]](#).
  - [4] P. Arias, D. Cadamuro, M. Goodsell, J. Jaeckel, J. Redondo, and A. Ringwald, *JCAP* **06**, 013 (2012), [arXiv:1201.5902 \[hep-ph\]](#).

- [5] P. W. Graham, J. Mardon, and S. Rajendran, *Phys. Rev. D* **93**, 103520 (2016), [arXiv:1504.02102 \[hep-ph\]](#).
- [6] M. Fabbrichesi, E. Gabrielli, and G. Lanfranchi, (2020), [10.1007/978-3-030-62519-1, arXiv:2005.01515 \[hep-ph\]](#).
- [7] P. Arias, A. Arza, B. Döbrich, J. Gamboa, and F. Méndez, *Eur. Phys. J. C* **75**, 310 (2015), [arXiv:1411.4986 \[hep-ph\]](#).
- [8] S. Chaudhuri, P. W. Graham, K. Irwin, J. Mardon, S. Rajendran, and Y. Zhao, *Phys. Rev. D* **92**, 075012 (2015), [arXiv:1411.7382 \[hep-ph\]](#).
- [9] L. H. Nguyen, A. Lobanov, and D. Horns, *JCAP* **10**, 014 (2019), [arXiv:1907.12449 \[hep-ex\]](#).
- [10] R. Cervantes *et al.*, *Phys. Rev. D* **106**, 102002 (2022), [arXiv:2204.09475 \[hep-ex\]](#).
- [11] R. Cervantes, C. Braggio, B. Giaccone, D. Frolov, A. Grassellino, R. Harnik, O. Melnychuk, R. Pilipenko, S. Posen, and A. Romanenko, (2022), [arXiv:2208.03183 \[hep-ex\]](#).
- [12] B. T. McAllister, A. Quiskamp, C. A. J. O’Hare, P. Altin, E. N. Ivanov, M. Goryachev, and M. E. Tobar, *Annalen Phys.* **536**, 2200622 (2024), [arXiv:2212.01971 \[hep-ph\]](#).
- [13] R. Cervantes *et al.*, *Phys. Rev. Lett.* **129**, 201301 (2022), [arXiv:2204.03818 \[hep-ex\]](#).
- [14] K. Ramanathan, N. Klimovich, R. Basu Thakur, B. H. Eom, H. G. LeDuc, S. Shu, A. D. Beyer, and P. K. Day, *Phys. Rev. Lett.* **130**, 231001 (2023), [arXiv:2209.03419 \[astro-ph.CO\]](#).
- [15] T. Schneemann, K. Schmieden, and M. Schott, (2023), [arXiv:2308.08337 \[hep-ex\]](#).
- [16] Z. Tang *et al.*, (2023), [arXiv:2305.09711 \[hep-ex\]](#).
- [17] D. He *et al.*, (2024), [arXiv:2404.00908 \[hep-ex\]](#).
- [18] P. A. M. Dirac, *Proc. Roy. Soc. Lond. A* **133**, 60 (1931).
- [19] T. T. Wu and C. N. Yang, *Phys. Rev. D* **12**, 3845 (1975).
- [20] G. ’t Hooft, *Nucl. Phys. B* **79**, 276 (1974).
- [21] A. M. Polyakov, *JETP Lett.* **20**, 194 (1974).
- [22] Y. M. Cho and D. Maison, *Phys. Lett. B* **391**, 360 (1997), [arXiv:hep-th/9601028](#).
- [23] P. Q. Hung, *Nucl. Phys. B* **962**, 115278 (2021), [arXiv:2003.02794 \[hep-ph\]](#).
- [24] J. Alexandre and N. E. Mavromatos, *Phys. Rev. D* **100**, 096005 (2019), [arXiv:1906.08738 \[hep-ph\]](#).
- [25] J. Ellis, N. E. Mavromatos, and T. You, *Phys. Lett. B* **756**, 29 (2016), [arXiv:1602.01745 \[hep-ph\]](#).
- [26] G. Lazarides and Q. Shafi, *Phys. Rev. D* **103**, 095021 (2021), [arXiv:2102.07124 \[hep-ph\]](#).
- [27] J. S. Schwinger, *Phys. Rev.* **144**, 1087 (1966).
- [28] D. Zwanziger, *Phys. Rev.* **176**, 1489 (1968).
- [29] D. Zwanziger, *Phys. Rev. D* **3**, 880 (1971).
- [30] R. A. Brandt, F. Neri, and D. Zwanziger, *Phys. Rev. Lett.* **40**, 147 (1978).
- [31] R. A. Brandt, F. Neri, and D. Zwanziger, *Phys. Rev. D* **19**, 1153 (1979).
- [32] A. V. Sokolov and A. Ringwald, *Annalen Phys.* **2023** (2023), [10.1002/andp.202300112, arXiv:2303.10170 \[hep-ph\]](#).
- [33] A. V. Sokolov and A. Ringwald, (2022), [arXiv:2205.02605 \[hep-ph\]](#).
- [34] B. Heidenreich, J. McNamara, and M. Reece, *JHEP* **01**, 120 (2024), [arXiv:2309.07951 \[hep-ph\]](#).

- [35] T. Li and R.-J. Zhang, (2023), [arXiv:2312.01355 \[hep-ph\]](#).
- [36] T. Li, R.-J. Zhang, and C.-J. Dai, *JHEP* **03**, 088 (2023), [arXiv:2211.06847 \[hep-ph\]](#).
- [37] M. E. Tobar, C. A. Thomson, B. T. McAllister, M. Goryachev, A. V. Sokolov, and A. Ringwald, *Annalen Phys.* **536**, 2200594 (2024), [arXiv:2211.09637 \[hep-ph\]](#).
- [38] T. Li, C.-J. Dai, and R.-J. Zhang, *Phys. Rev. D* **109**, 015026 (2024), [arXiv:2304.12525 \[hep-ph\]](#).
- [39] T. Li and R.-J. Zhang, *Chin. Phys. C* **47**, 123104 (2023), [arXiv:2305.01344 \[hep-ph\]](#).
- [40] M. E. Tobar, A. V. Sokolov, A. Ringwald, and M. Goryachev, *Phys. Rev. D* **108**, 035024 (2023), [arXiv:2306.13320 \[hep-ph\]](#).
- [41] A. Patkos, *Mod. Phys. Lett. A* **38**, 2350137 (2023), [arXiv:2309.05523 \[hep-ph\]](#).
- [42] C.-J. Dai, T. Li, and R.-J. Zhang, (2024), [arXiv:2401.14195 \[hep-ph\]](#).
- [43] J. Schwinger, *Phys. Rev.* **152**, 1219 (1966).
- [44] J. S. Schwinger, *Phys. Rev.* **158**, 1391 (1967).
- [45] J. S. Schwinger, *Phys. Rev.* **173**, 1536 (1968).
- [46] M. S. Turner, *Phys. Rev. D* **42**, 3572 (1990).
- [47] C. Bartram *et al.* (ADMX), *Phys. Rev. Lett.* **127**, 261803 (2021), [arXiv:2110.06096 \[hep-ex\]](#).
- [48] A. V. Dixit, S. Chakram, K. He, A. Agrawal, R. K. Naik, D. I. Schuster, and A. Chou, *Phys. Rev. Lett.* **126**, 141302 (2021), [arXiv:2008.12231 \[hep-ex\]](#).
- [49] T. Braine *et al.* (ADMX), *Phys. Rev. Lett.* **124**, 101303 (2020), [arXiv:1910.08638 \[hep-ex\]](#).
- [50] C. O’Hare, “cajohare/axionlimits: Axionlimits,” <https://cajohare.github.io/AxionLimits/> (2020).
- [51] J. Duan, Y. Gao, C.-Y. Ji, S. Sun, Y. Yao, and Y.-L. Zhang, *Phys. Rev. D* **107**, 015019 (2023), [arXiv:2206.13543 \[hep-ph\]](#).
- [52] A. Phipps *et al.*, *Springer Proc. Phys.* **245**, 139 (2020), [arXiv:1906.08814 \[astro-ph.CO\]](#).
- [53] N. Crisosto, P. Sikivie, N. S. Sullivan, D. B. Tanner, J. Yang, and G. Rybka, *Phys. Rev. Lett.* **124**, 241101 (2020), [arXiv:1911.05772 \[astro-ph.CO\]](#).
- [54] B. Godfrey *et al.*, *Phys. Rev. D* **104**, 012013 (2021), [arXiv:2101.02805 \[physics.ins-det\]](#).
- [55] J. Levine, B. Godfrey, J. A. Tyson, S. M. Tripathi, D. Polin, A. Aminaei, B. H. Kolner, and P. Stucky, (2024), [arXiv:2405.20444 \[hep-ex\]](#).